GA–A25394

EDGE TRANSPORT BARRIERS IN MAGNETIC FUSION PLASMAS

by
P. GOHIL

MARCH 2006

GENERAL ATOMICS

DISCLAIMER

GA–A25394

EDGE TRANSPORT BARRIERS IN MAGNETIC FUSION PLASMAS

by
P. GOHIL

This is a preprint of a paper to be submitted for publication in *Compte-Rendu de l'AcadÈmie des Sciences.*

Work supported by
the U.S. Department of Energy under
DE-FC02-04ER54698

GENERAL ATOMICS PROJECT 30200
MARCH 2006

Abstract

The present level of understanding of the physics of the formation and sustainment of edge transport barriers in magnetically confined fusion plasmas is presented. The formation of edge transport barriers is studied through evolution of mechanisms which can suppress plasma turbulence and so reduce turbulent driven transport, such as $E \times B$ flow shear stabilization of turbulence. Comparisons of theoretical studies with experimental results are described including investigations of zonal flows, which are considered important for saturation and self-regulation of turbulence and turbulence-driven transport. Processes that affect the dynamics and spatial structure of the edge barrier are described with emphasis on the width of the transport barrier.

I. INTRODUCTION

In magnetically contained fusion plasmas, the transition from a low energy confinement state, known as low (L) mode, to a significantly higher energy confinement state, known as high (H) mode, is marked by the formation of a transport barrier at the plasma edge. This so-called H-mode edge transport barrier (ETB) was first discovered in 1982 in the ASDEX device [1] and since then has been reproduced in a wide range of magnetic confinement fusion devices such as divertor and limiter tokamaks, mirror machines and stellerators. The robust and ubiquitous nature of the H-mode ETB, and the associated energy confinement improvement, makes it an important ingredient for any device aiming to achieve sustained burning plasma conditions. For example, the standard operating regime for the International Thermonuclear Experimental Reactor (ITER) [2] requires the production and sustainment of the H-mode ETB.

The edge transport barrier, which is located just inside the last closed magnetic flux surface (LCFS), represents a sharp and abrupt change in transport which results in steep gradients of ion and electron densities and temperatures. Understanding the physics of the formation, sustainment and destruction of these edge transport barriers can significantly advance efforts towards achieving reactor relevant plasma conditions. Barrier formation can result from a reduction in transport at the plasma edge. Since edge transport is primarily turbulent, a reduction in this turbulent transport is therefore necessary for barrier formation. Consequently, understanding the physics of barrier formation often requires determining mechanisms for transport reduction via stabilization of turbulence.

This paper is not intended to be a comprehensive review of edge transport barriers, but rather an introductory overview that directs the reader to relevant research in this field. Mechanisms for the stabilization of turbulence will be discussed in Section II. The dynamics, sustainment and structure of the ETB is covered in Section III and Section IV contains the conclusions.

II. FORMATION OF THE EDGE TRANSPORT BARRIER

A. Stabilization mechanisms

A requirement for transport barrier formation is the reduction of fluctuation driven transport. This can most frequently be achieved by stabilization or decorrelation of microturbulence in the plasma. Understanding the transport barrier formation then requires determining mechanisms which can suppress turbulent modes. The stabilization mechanisms have to account for the different dynamic behaviors of the various species in the plasma. Also, the spontaneous transition from L-mode to H-mode confinement (the L-H transition) in fusion plasmas requires sufficient heating power for its production. The actual heating power required can depend on different plasma and device parameters such as toroidal field, density and plasma size. Furthermore, since the L-H transition is essentially a plasma edge phenomena, local plasma parameters, scale lengths and atomic processes have a bearing on the transition physics and threshold power requirements. All these factors need to be considered by theories attempting to explain the ETB formation as well as also being applied to tests of the theories themselves.

Various theories have been put forward to explain the L-H transitiion. One set of theories are based on the suppression of turbulent transport by sheared radial electric fields or plasma flow [3, 4, 5, 6, 7, 8]. This can be achieved either by stabilization of linear modes or as a result of a reduction in correlation lengths or turbulence amplitudes or by phase changes between fluctuations responsible for the turbulent transport. Another set of theories are based on producing the right set of edge plasma conditions required for stabilization of certain instabilities. Such theories invoke ideal magnetohydrodynamic (MHD) ballooning mode stability [9, 10] or peeling modes [11, 12] to explain the L-H transition, in which stability to the ballooning or peeling modes leads to barrier formation. Other theories invoke ideal and drift resistive ballooning modes in which diamagnetic effects cause stabilization of such modes leading to bifurcation in the edge transport [13, 14, 15]. Stabilization of drift resistive ballooning modes in a toroidal geometry have been studied using 3D nonlinear simulations [16, 17]. These theories rely on an increase in the edge temperature to stabilize the resistive ballooning mode leading to

turbulence suppression and barrier formation. Another set of theories have studied collisional drift wave turbulence [18, 19] and drift-Alfvén turbulence at the plasma edge [20, 21, 22]. Again, stabilization of these modes and the subsequent L-H transition are related to the edge temperature and edge β.

Given that many L-H transition theories rely on changes in certain edge parameters to affect the edge turbulence and so lead to the H-mode transition, it should be possible to quantatively test these theories with experimental data. The theories based on MHD ballooning modes are inconsistent with experimental data from DIII-D and ASDEX Upgrade [23, 24] which indicate that the H-mode transition is produced for edge pressures below the MHD ballooning limit and in cases which do not attain access to the second stability regime. Experimental data from COMPASS-D [12, 25] has been compared favorably with the peeling mode model [12], which was used to explain the increased difficulty in obtaining H-mode transitions at low edge collisionality in that tokamak. However, experimental data from DIII-D on experiments with H-mode transitions triggered by pellet injection [26] contradict this model since H-mode transitions are obtained at low edge pressure gradients far below the theoretical predictions.

The drift resistive ballooning model [13, 14, 15] evolved to the point of predicting the formation of the edge transport barrier when the MHD ballooning parameter, α, and a diamagnetic parameter, α_{diam}, exceeded certain critical values of, typically, $\alpha \geq 0.5$ and $\alpha_{diam} \geq 0.5 - 0.75$ (depending on machine parameters). Here $\alpha = -Rq^2 d\beta/dr$ and $\alpha_{diam} = V_{di} t_o / L_o$, where $V_{di} = \rho_s c_s / L_{\rho_i}$, $\rho_s = c_s / \Omega_{ci}$. Here q is the plasma safety factor, β is the ratio of the plasma pressure to the magnetic pressure, R is the major radius, c_s is the ion speed, Ω_{ci} is the ion cyclotron frequency, t_o is the ideal ballooning time, L_o is a characteristic turbulence scale length and L_{pi} is the ion pressure scale length. Good agreement was found between this model and H-mode transition data from Alcator C-Mod [27] with regard to these two parameters. Data from DIII-D [28] and COMPASS-D [29] show relatively good agreement with the ballooning parameter, α, but completely fail to correlate with α_{diam}. Furthermore, pellet triggered H-mode transition results from DIII-D [26] exhibit no correlation with either parameter, α or α_{diam}, at barrier formation. The drift-Alfvén turbulence model [20, 21] relies on increased edge pressure

gradients to lead to the Alfvén waves mixing with the electron drift waves and thereby stabilizing the long wavelength turbulence. This model shows some agreement with ASDEX Upgrade data [30, 31], but, once again, there is no agreement with the DIII-D experimental results on H-mode transport barriers formed with pellet injection [26].

A further mechanism for edge turbulence stabilization is that by $E \times B$ flow shear nonlinear decorrelation of turbulence [6, 8] which developed from early work that emphasized E_r as the stabilizing element [4, 32]. Here E_r is the radial electric field at the plasma edge and B is the toroidal magnetic field. For decorrelation of turbulence, the $E \times B$ shearing rate, $\omega_{E\times B}$, must be comparable to the nonlinear turbulence decorrelation rate, $\Delta\omega_D$, in the absence of $E \times B$ velocity shear [6]. An expression for the $\omega_{E\times B}$ shearing rate for flute-like modes in the toroidal geometry is given by [43]

$$\omega_{E\times B} = \frac{RB_\theta}{B}\frac{\partial}{\partial r}\left(\frac{E_r}{RB_\theta}\right) \quad , \tag{1}$$

where R is the plasma major radius, B_θ is the poloidal magnetic field and E_r is the radial electric field which is given by the radial force balance equation for any plasma species, i, by

$$E_r = \frac{\nabla p_i}{n_i Z_i e} + v_{\phi\, i} B_\theta - v_{\theta\, i} B_\phi \quad , \tag{2}$$

where n is the species density, p is the pressure, z is the charge number, e is the electric charge, v_ϕ is toroidal rotation, v_θ is the poloidal rotation, B_ϕ is the toroidal magnetic field.

This work further developed into approximate expressions for quenching unstable ITG modes [33], whereby the turbulence is completely suppressed when the $E \times B$ shear rate, $\omega_{E\times B}$, exceeds γ_{max}, where γ_{max} is the maximum linear growth rate of all the instabilities without $\omega_{E\times B}$. Note that transport barrier can also be formed in the plasma interior (i.e., internal transport barriers, ITBs) and that linear stabilization of turbulent modes [7, 34, 35] has shown great relevance in the plasma core where spatial and temporal correlation has been observed between increased $E \times B$ velocity shear and reduction in the core turbulence and the formation of ITBs (e.g. in DIII-D [36, 37, 38], in JET [39, 40] in TFTR [41, 42]. In physical terms, it is the gradient or

shear in the $E \times B$ velocity that reduces the radial correlation length of the turbulent eddies in the plasma due to both a change in the phase relationship between the density and velocity perturbations as well as to decreases in the amplitude of the turbulent fluctuations. In the case of linear stabilization, the $E \times B$ velocity shear leads to increased stability by coupling the unstable modes to nearby stable modes. An important feature of $E \times B$ velocity shear stabilization are feedback loops involving the various terms (i.e., ∇P, ϑ_θ, ϑ_ϕ) of Eq. (2) which can lead to further increasing the values of E_r and $\omega_{E\times B}$ and, thereby, maintaining the effectiveness of $E \times B$ velocity shear stabilization. Note that, although internal transport barrier formation requirements will not be discussed in this paper, $E \times B$ velocity shear stabilization is the only turbulence suppression mechanism that can explain the formation of both the ETB and the ITB i.e., barrier formation at any radial location in the plasma.

Because the edge transport barrier, by definition, is localized just inside the last closed magnetic flux surface, a large number of plasma diagnostic systems can be brought to bear at this specific location in the plasma for fast, highly spatially resolved measurements of the barrier. This is important in order to accurately diagnose the clear simultaneous barriers formed in the n_e, T_e, and T_i profiles and their relationship to other plasma quantities such as the E_r profiles. For example, DIII-D high spatial measurements have revealed that the width of the well-like E_r structure formed at the plasma edge at barrier formation is $\sim$1 cm and is invariant to a large range of plasma parameters [44].

Also, in DIII-D, detailed measurements of edge temperature and density profiles, edge E_r profiles and fluctuations have revealed important details of turbulence behavior and the role of E_r for edge barrier formation. These studies have revealed: (a) changes in E_r occur prior to the H-mode barrier formation [45, 46, 47]; (b) there is a dramatic reduction in edge density fluctuations and fluctuation-driven particle flux coincident with barrier formation [46, 48]; (c) fluctuations are reduced and the transport barrier forms in the region of steep E_r gradient [49]; (d) the radial correlation length decreases at the H-mode barrier formation [50]; (e) $\omega_{E\times B}$ is comparable to the turbulence decorrelation rate, $\Delta\omega_D$, in L-mode, but increases significantly

across the transition from L-mode to H-mode and $\omega_{E\times B}$ is much greater than $\Delta\omega_D$ in H-mode [51]; (f) the edge $\omega_{E\times B}$ shearing rate is sufficient for effective suppression of turbulence as defined by the criterion of Ref. [6] for a large range of operational configurations and operating parameters [44]. Figure 1 shows the fast changes in the edge E_r profile at ETB formation observed in DIII-D [47]. Very fast time resolution measurements of E_r at ETB formation have been made on JFT-2M [52, 53, 54]. Figure 2 shows heavy ion beam probe (HIBP) measurements of the edge electrostatic potential and local density fluctuations at the ETB formation in JFT-2M [54]. The HIBP diagnostic has the advantage of being able to make local electrostatic potential and fluctuation measurements simultaneously with fast time resolution ($\sim$2 μs). Observations of clear changes in E_r at the edge barrier formation have also been made in COMPASS-D [55], ASDEX [56], the W7-AS stellerator [57] and the H-1 heliac [58]. The above results are consistent with $E \times B$ velocity shear causing reduction in fluctuations and, thereby, leading to the formation of the transport barrier.

The above cases of ETB formation are for spontaneously produced barriers in which some level of edge heating (e.g. ohmic, sawteeth heat pulse, auxiliary) occurs. However, edge transport barriers have also been produced by directly biasing the plasma edge with an electric field applied through an electrode as in CCT [59] TUMAN-3 [60] and TEXTOR [61, 62, 63]. Figure 3 shows Langmuir probe measurements from TEXTOR indicating a clear reduction in the temperature fluctuations with increased shear in E_r applied by an electrode inserted at the plasma edge [62]. Further experimental results from TEXTOR [63, 64] show that the changes in electron density and improvements in particle confinement are both spatially and temporally correlated with changes in ∇E_r and address the fundamental issue of causality. Figure 4 shows the temporal behavior of these changes where oscillations in the applied voltage produce oscillation in ∇E_r. The oscillations in ∇E_r cause oscillations in ∇n_e with the ∇E_r oscillations preceding the oscillations in ∇n_e by about 4-6 ms. The fact that changes in ∇E_r lead to changes in ∇n_e is a clear demonstration of $E \times B$ shear directly affecting transport.

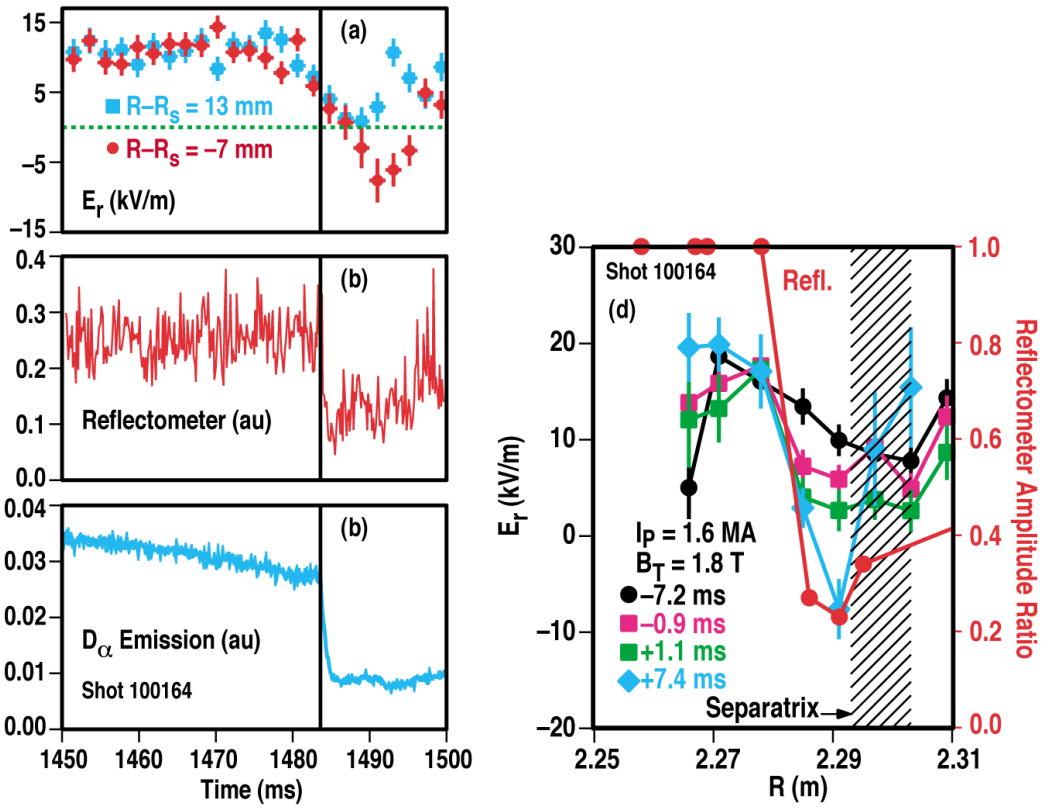

Fig. 1. Temporal and spatial changes in several edge quantities at the formation of the ETB in DIII-D. (a) The radial electric field, E_r, at two locations (inside and outside the last closed flux surface), (b) the density fluctuation, (c) the D_α emission at the divertor, and (d) the E_r profile and the density fluctuations at the plasma edge. The edge E_r and the density fluctuations are measured using charge exchange recombination spectroscopy and reflectometry, respectively. The reflectometer amplitude ratio represents the ratio of the fluctuation amplitudes before and after the formation of the ETB. Note that (a) shows changes in E_r just prior to the decrease in the edge density fluctuations and the D_α signal and (d) shows a substantial reduction in the density fluctuations in the same region where a large shear in E_r develops [47]. *[Reprinted courtesy of K.H. Burrell, Rev. Sci. Instrum.* ***72****, 906 (2001), American Institute of Physics.]*

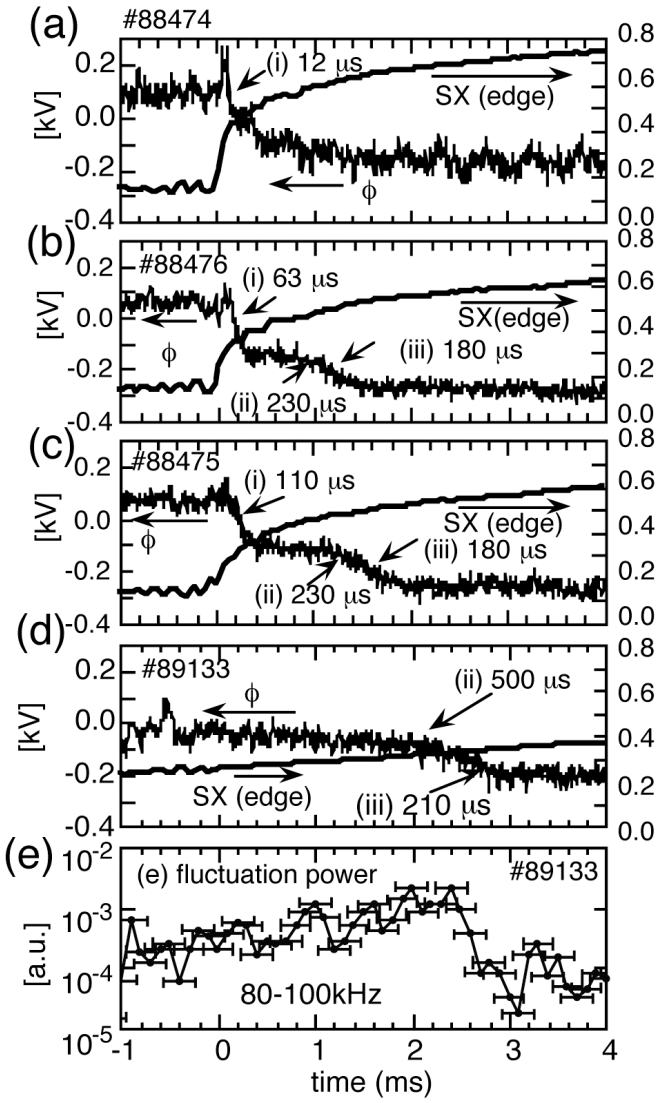

Fig. 2. Temporal behavior of the potential change near the separatrix and the edge SX intensity. (a-c) show the case of $P_{in} > P_{th}$ and (d) shows the case of $P_{in} \sim P_{th}$. The times shown are the characteristic times from the exponential drop. (e) Temporal behavior and the fluctuation power in the case of $P_{in} \sim P_{th}$ [the same shot as in (d)]. The zero on the horizontal axis indicates the time of the arrival of a sawtooth heat pulse at the edge [54]. *[Reprinted courtesy of Y. Miura, et al., Nucl. Fusion **41**, 937 (2001), Institute of Physics.]*

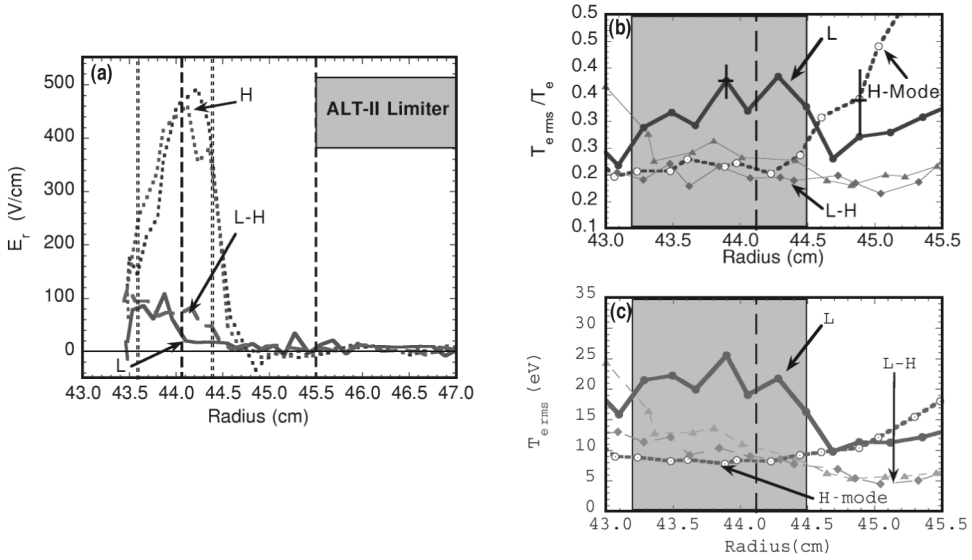

Fig. 3. (a) Profiles of the radial electric field for L-mode, L-H (transition from low to high confinement) and H-mode. The long-dashed and dotted lines mark the maximum of the radial electric field and its derivative respectively. (b,c) Profiles of the normalized and absolute temperature fluctuation, $\tilde{T}_e$, respectively, for L-mode, L-H transition and H-mode. The shaded region represents the E_r shear layer defined from (a) [62]. *[Reprinted courtesy of J.A. Boedo, et al., Phys. Rev. Lett.* ***84****, 2630 (2000), American Institute of Physics.]*

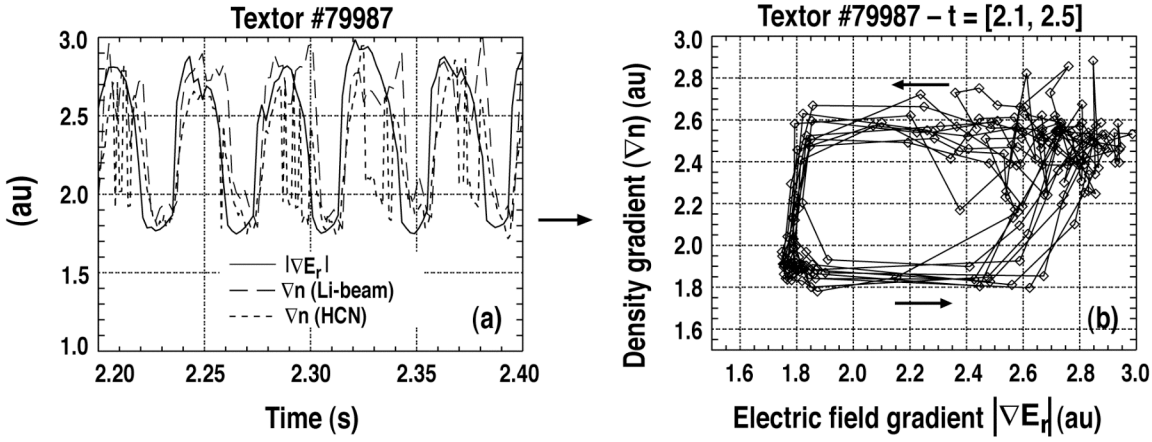

Fig. 4. Time history of the maximum gradient of the radial electric field, ∇E_r, and the electron density gradient, ∇n_e, for a biased electrode H-mode in the TEXTOR tokamak. (b) Hysteresis diagram of ∇E_r versus ∇n_e for the data shown in (a). The time resolution of the E_r and n_e measurements are 0.04 ms for E_r, about 2 ms and 0.02 ms for the n_e measurements by the lithium beam and HCN laser systems, respectively. The direction of the arrows in (b) indicate increasing time and show that changes in ∇E_r precede changes in ∇n_e [63,64]. *[Reprinted courtesy of K.H. Burrell, et al., Phys. Plasmas* ***6****, 441 (1999), American Institute of Physics.]*

Another example of causality and $E \times B$ shear affecting turbulent transport are the cases of very high (VH)-mode discharges in DIII-D [65, 66]. The VH-mode contains an edge transport barrier that extends deeper into the plasma than in an H-mode and correspondingly achieves even greater levels of confinement. Tests of the influence of $E \times B$ velocity shear on confinement were performed by varying the toroidal rotation in these plasmas through the use of magnetic braking [67, 68]. These experiments showed that the amplitude of density fluctuations and transport rates increased as the $E \times B$ shearing rate decreased and vice versa [45, 68].

All the above indicate that there is a considerable amount of experimental results that show the clear reduction of turbulent transport due to $E \times B$ flow shear. However, the origin of the sheared flows in spontaneously produced H-mode transitions (i.e., produced by heating the plasma) has yet to be resolved. Theoretical models have proposed mechanisms such as neoclassical ion-orbit loss [8], Stringer spinup of poloidal flow [69], and shear flow driven by turbulent Reynold's stress [70] in a nonlinear organized manner [71]. Experimental results from DIII-D [72] have showed that the direction of rotation of the majority ion species is inconsistent with ion-orbit loss mechanisms. As yet, no clear measurements of the Stringer spinup of poloidal flow have been made. The issues of self-organization and turbulence-generated (zonal) flow shear have been addressed in several experiments and these will be discussed in the next section.

B. Zonal flows

Zonal flows are considered important for saturation and self-regulation of turbulence and turbulence-driven transport. Zonal flows can be self-generated by turbulence through Reynold's stress [70, 71, 73] and, because their radial scale ranges from the radial scale of turbulent eddies up to the device size, they can be very effective in suppressing turbulence. In this self-generation mechanism, the energy source for the zonal flows comes from the nonlinear coupling with the turbulence, whilst the total energy is conserved. There are two broad classes of zonal flows. One is a low frequency zonal flow with purely radial variation of the electrostatic potential oscillation and so with toroidal, n, and poloidal mode, m, numbers of zero (i.e., $n = 0$, $m = 0$)

and a finite radial wave number, k_r. A second type of zonal flow of higher frequency is called the geodesic acoustic mode (GAM) which also has basically no toroidal or poloidal phase variation but oscillates at a specific frequency. Because the GAMs are damped by ion-Landau damping [74] or turbulence viscosity [75], they play a greater role at the plasma edge where the damping rate is lower [73]. Note that zonal flows have been measured in the plasma core of CHS [76, 77] with the use of a dual-HIBP system through determination of the cross-coherence of E_r at different plasma radii from which the radial wavelength of the zonal flow has been evaluated.

In the case of the edge transport barrier, the signature of Reynold's stress-driven flow shear has been determined from three-wave coupling (bicoherence) of potential fluctuations measured across the L-H transition in DIII-D using a reciprocating Langmuir probe [78, 79]. These results indicate that the bi-coherence between low and high turbulence frequencies increases just before the L-H transition and before the reduction in plasma turbulence. The transition in bi-coherence occurs in the region of increased $E \times B$ velocity shear at the L-H transition and decays a few milliseconds after the L-H transition. These results are consistent with a transient Reynold's stress-driven zonal flow shear [73, 80]. Also, poloidal flow induced by Reynold's stress has been measured in the HT-6M tokamak [81]. The radial profile of the electrostatic Reynold's stress has been measured in the plasma boundary region of the ISSTOK tokamak [82], the CSDX helicon device [83], the HT-7 tokamak [84], and the Extrap-T2R reversed field pinch [85]. Also, theory-based calculations of zonal flow generation by finite β drift waves have found good agreement with experimental data from DIII-D [86].

Measurements of density fluctuations at or near the plasma edge have been used for estimation of the zonal flow. In JFT-2M, Langmuir probe and HIBP measurements at the plasma edge have revealed feedback loops between the zonal flows and the GAMs [87, 88]. GAMs have been identified from studies of turbulence velocities performed on DIII-D using beam emission spectroscopy (BES) for 2-D measurements of the density fluctuations in L-mode plasmas [89]. Further evidence of GAMs has been obtained on ASDEX Upgrade, where the poloidal velocity of the plasma turbulence has been measured using Doppler reflectometry in L-mode plasmas

[Fig. 5(a)] [90]. Frequency analysis of these measurements indicates that the frequency of the velocity oscillations varies as $(T_e + T_i)^{1/2}$which is consistent with the theoretical predictions [73] whereby $\omega_{GAM} = G[(T_e + T_i)/m_i]^{1/2}/R$ where T_i and T_e are the ion and electron temperatures, respectively, G is a geometrical factor of order unity, m_i is the ion mass, and R is the plasma major radius. The location of the coherent velocity oscillations is observed to be in the steep density gradient at the plasma edge which disagrees with DIII-D and JFT-2M results (see below and Fig. 6). Further BES measurements on DIII-D also reveal a temperature dependence [Fig. 5(b)] for the coherent oscillations [91, 92] consistent with theoretical predictions for the GAM, similar to the ASDEX Upgrade observations. The radial profile of the GAM amplitude has been determined from BES measurements and repeat L-mode discharges to allow a more thorough mapping of the radial structure [93]. Figure 6(a) shows the radial profile of the GAM amplitude overlaid with the edge q profile. The GAM amplitude is seen to decrease into the plasma core (i.e., at smaller q values) and this is qualitatively consistent with the q scaling for Landau damping [74]. Also shown are results from the JFT-2M tokamak [Fig. 6(b)] indicating the spatial structure of the GAM at the plasma edge in L-mode determined from HIBP measurements [94]. Both sets of results are very similar indicating some level of commonality at the plasma edge and again stressing that they are clearly an important edge phenomena. These experimental data show the existence of zonal flows and GAMs in L-mode plasmas, which then could be the trigger mechanisms for the large $E \times B$ flow shear observed at the L-H transition.

These results are encouraging for understanding edge turbulence behavior and further studies of these modes is required to determine how they can be used to control turbulent transport at the edge and so provide a predictive capability for barrier formation.

C. Critical parameters for the barrier formation

The fact that some level of additional heat flux at the plasma edge is usually required for the spontaneous formation of ETBs indicates that some threshold requirement (power or otherwise) has to be satisfied for the

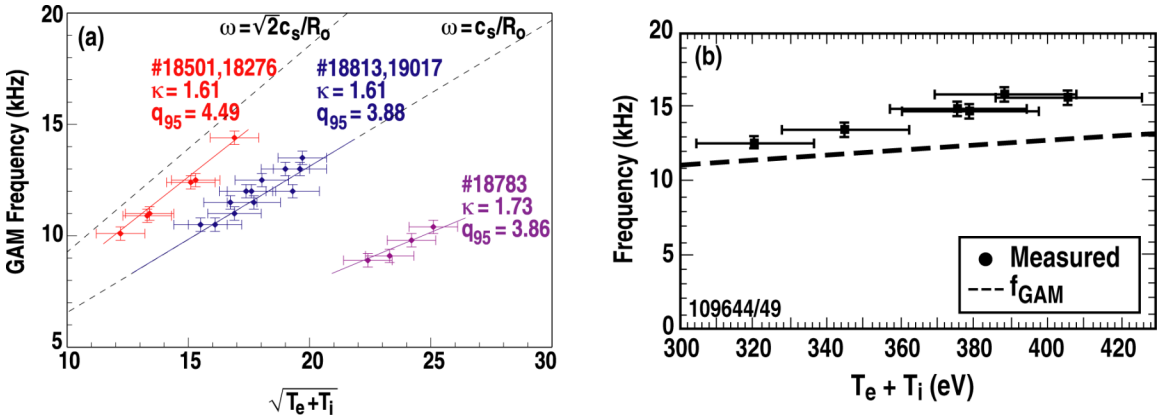

Fig. 5. The frequency of the GAM as a function of the local electron and ion temperatures for ASDEX Upgrade and DIII-D. (a) GAM frequency versus $(T_e + T_i)^{1/2}$ for ASDEX Upgrade for different elongation, κ and q_{95} values; (b) the GAM frequency versus $T_e + T_i$. Both sets of data exhibit the same scaling of the frequency with temperature expected from theoretical predictions [90,92]. *[(a) Reprinted courtesy of G. Conway, et al., Proc. 31st EPS Conf. on Controlled Fusion and Plasma Physics, London, United Kingdom (Euro. Physical Society, 2004) paper P4.124; (b) Reprinted courtesy of G.R. McKee, et al., Plasma Phys. Control. Fusion **45**, A477 (2003), Institute of Physics.]*

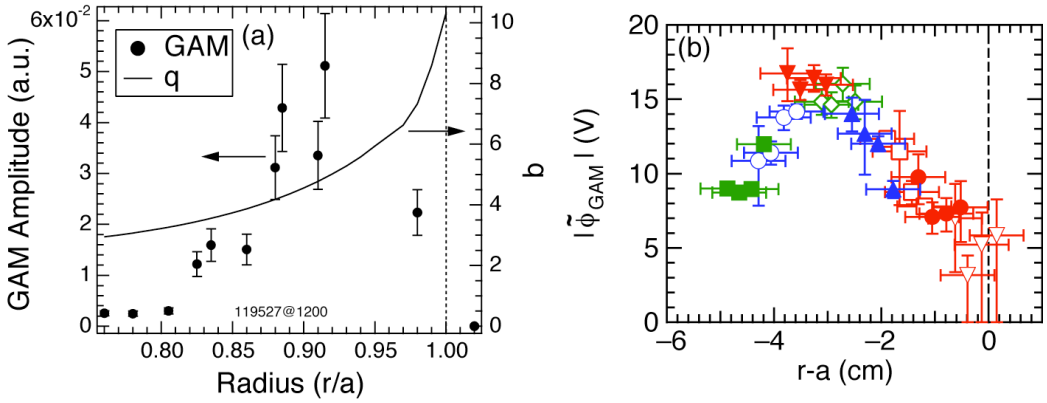

Fig. 6. Radial profile of the GAM amplitude at the plasma edge in (a) DIII-D and (b) JFT-2M showing strong peaking just inside the separatrix [93,94]. *[Reprinted courtesy of G.R. McKee, et al., Plasma Phys. Control. Fusion **48**, S123 (2006), Institute of Physics; T. Ido, et al., Plasma Phys. Control. Fusion **48**, S41 (2006), Institute of Physics.]*

formation process. Can this threshold requirement then be reflected in some critical plasma parameters required for ETB formation? In C-Mod, the ETB is formed at certain threshold values of the edge electron temperature or edge temperature gradient [95]. Similarly in JET, the attainment of threshold values of the electron and ion temperature at the plasma edge are required for ETB formation [96, 97]. However, results from DIII-D with pellet triggered ETBs indicate that the simple edge temperature (electron or ion) is not a critical parameter in behavior formation since the edge temperatures are significantly reduced at pellet injection [26]. The determination of critical edge parameters is further complicated by the fact that the ETB power threshold can be strongly dependent on machine parameters, such as magnetic field and plasma size and shape [98] and also on the plasma or divertor configuration and the direction of the ion ∇B drift with respect to the divertor X-point position [99]. For example, the threshold power in MAST is reduced for the double-null configuration [100] whereas, in NSTX, a lower threshold power is obtained with single-null operation [101]. Variations in the threshold power (by a factor of two) have been observed in DIII-D depending on the direction of the ion ∇B drift ralative to the X-point [99]. Further to this, the density of neutral particles at the edge can affect the threshold power as pointed out for DIII-D and JT-60U [102, 103]. Also, the location of the neutral particle input can affect the threshold. For example, the threshold power for the ETB is reduced when gas is injected from the high field side instead of the low field side in MAST [100] and NSTX [101].

Attempts have been made to produce a power threshold scaling law from a set of machine and plasma parameters using a multi-machine database [98, 104]. However, as pointed out above, the threshold power can be significantly affected by many variables, including the plasma configuration and also atomic processes at the plasma edge. Therefore, there remain large uncertainties in predictions for the power threshold for the ETB formation for present and future devices. Furthermore, this large variability is reflected in the inability to determine the critical edge plasma parameters important for the ETB formation. Correspondingly, there has been great difficulty in producing a comprehensive theory-based model for the ETB formation which can be used for predictive capabilities. Improved edge measurements will

help in resolving this issue as well as more experiment-theory comparisons of theories with measurable quantities.

In summary, the importance of $E \times B$ sheared flow in the physics of the formation of the edge transport barrier has now been well-established, as described in Sec. II.A. The trigger mechanisms for generation of the sheared flow are as yet unresolved. Indeed, the fast bifurcations in edge quantities, such as E_r, imply some nonlinear process that can occur on sub-millisecond timescales. Turbulent stresses and zonal flows could play important roles in these mechanisms especially given their influence in the self-regulation of drift wave turbulence and transport. It should also be noted that different trigger mechanisms could be involved for different plasma conditions.

Further work is therefore needed in the determination of these rapid bifurcation mechanisms which ultimately requires development of edge diagnostic systems capable of even greater (e.g. by more than an order of magnitude) spatial and temporal resolution. These measurements then need to be used for evaluations of theory-based predictive models of the ETB. This is a challenge for experimental and theoretical investigations in this area, but clearly one that must be met for further significant advances to be made in this area.

III. DYNAMICS AND STRUCTURE OF THE ETB

The spatial structure of the ETB is of vital importance for the energy confinement and fusion gain of the whole plasma. Because of so-called stiffness [105, 106] of the temperature profile, the energy confinement enhancement over L-mode conditions increases with increasing temperature and pressure at the edge pedestal (i.e., the location of the inboard edge of the ETB) [107]. Core profile stiffness is also predicted theoretically from models of turbulent transport [108, 109]. Since the edge pressure gradients are limited by MHD instabilities (see later), the pedestal pressure is then dependent on the width of the transport barrier. The issue then becomes one of understanding the physics that determines the width of the edge transport barrier. This section describes details of the mechanisms that affect the temporal and spatial characteristics of the ETB once it has formed.

As described previously, the physics of the formation of the ETB can be related to the suppression of edge turbulent transport by $E \times B$ flow shear. However, once the ETB has been formed, the physics of its sustainment and destruction can be influenced by several mechanisms, with the most notable being MHD instabilities. This is because the reduced transport and high plasma confinement achieved through the formation of the transport barrier produce large edge pressure gradients, which can drive MHD instabilities that often degrade or destroy the barrier. These instabilities are called edge localized modes (ELMs), which produce repeating cycles of destruction of the edge barrier. Due to space constraints, a detailed description of the ELM properties will not be presented, but the reader is directed to reviews of ELMs [110, 111]. ELMs can be beneficial to the overall longevity of the ETB as a result of the periodic degradation of the barrier which limits the increase of density and impurities in the plasma. Otherwise, the barrier would be irreversibly destroyed through excessive radiative power loss caused by the buildup of density and impurities in the plasma. However, it is the effects that the ELMs have on the divertor surfaces that make them detrimental. The large energy loss at the plasma edge due to the ELMs can lead to severe erosion of the divertor surfaces.

The dynamics of the ELM crashes [with onset times of the order of milliseconds] are based on large transient convective losses of energy and particles into the scrape-off layer (SOL) as a result of hitting an MHD stability limit. The physics of Type I ELMs are believed to be the result of coupled peeling-ballooning modes [11, 112, 113]. The large pressure gradients that develop in the ETB can cause ballooning modes to be driven unstable, whereas, the peeling mode is driven unstable by the edge current density (or its gradient). Both these drives are operative at the plasma edge and ultimately the pressure gradient is limited by the ideal MHD modes with an intermediate n, typically $n \sim 6 - 12$, where both the pressure gradient and current density are effective in destabilizing the modes. The ELM crash is a nonlinear process and a nonlinear theory for the ballooning mode has been constructed that predicts that the mode evolves into a narrow twisting flux tube, which rapidly erupts into the scrape-off layer [114, 115]. This model aims to explain the nonlinear evolution and rapid growth of the ELM. Experimental observations of such tube-like structures have been made on MAST [100, 116]. Figure 7 shows these filamentary structures, generated on a 100 μs time scale, which erupt on the outboard plasma side and which are in agreement with the above theory.

Some level of ELM control is required in order to mitigate the effects of ELMs on divertor erosion and for ITB compatibility whilst also maintaining a sufficient pedestal pressure for adequate burning plasma performance. ELM control has been achieved by: (a) pellet injection, whereby ELMs are induced by injecting small pellets at higher frequencies (pellet pacing) than the natural frequency of Type I ELMs as in ASDEX Upgrade and JT-60U [117, 118], (b) by applying an external magnetic field to apply a resonant magnetic perturbation to the plasma edge as in DIII-D [119, 120]; (c) by changing the toroidal rotation velocity as in JT-60U [144]; (d) by changing the edge current as in COMPASS-D and TCV [122, 123]. These techniques have shown some success for ELM control in present devices, but more progress is required to show they can be effectively applied to future burning plasma devices.

The strength and structure of the ETB is dependent on the ELM activity. The peeling-ballooning mode model can be used for predictions of the maximum pressure gradient expected in next-step fusion devices such as

ITER. This approach, together with the use of dimensionless parameters, has been used with inter-machine pedestal measurements to determine scaling of the transport barrier width [124]. A more theory-based approach using turbulent transport models applied across the pedestal region may provide a better understanding of the ETB structure [125] and will be used for future comparisons with multi-machine data.

The scaling of the transport barrier width, w_E, can also be evaluated from theories invoking stabilization of turbulence by E_r shear since the region of stabilization should be defined by the spatial extent of the flow shear. This then involves mechanisms affecting the radial electric field such as: (a) ion-orbit loss, where $w_E \propto \rho_{pi}$ (the ion poloidal gyroradius); (b) the influence on ion orbit-losses by neutral particles through charge exchange collisions and on the flow shear by poloidal flow damping [126, 127], so $w_E \propto \ell_n$ (the neutral penetration length); (c) viscosity, whereby $w_E \sim [\rho_{pi}^2 + (\mu_\perp/\nu_i)]^{1/2}$ where $\mu_\perp$ is the cross-field viscosity and ν_i represents poloidal flow damping [128]. Experimental results from JT-60U [129] indicate that $w_E \propto \rho_{pi}$ (Fig. 8), including the effects of ion orbit squeezing [131, 132] where the orbits are squeezed (or reduced) by the radial electric field shear. However, although data from DIII-D [130] are near the predicted values, they show no clear correlation with ρ_{pi}, while JET shows a weak scaling with ρ_{pi} [133]. Data from JFT-2M [134] indicates a weak response to ρ_{pi} and an influence of $\mu_\perp$. Overall, these results suggest that there is presently inconclusive evidence for the transport barrier width to be set by the ion orbit loss mechanism. With regard to the influence of neutral particles, multi-machine comparison experiments [124] suggest that the temperature ETB width is not governed by the neutral penetration. However, data from DIII-D indicates that the width of the edge electron density barrier appears to be correlated with the neutral penetration legnth [135].

Another approach to predicting the ETB width is to apply the mechanisms of turbulent transport models [136, 137] to the suppression of ITG modes at the plasma edge which then gives an expression for the ETB width [130] as $w_E \propto \rho_{*s}$, where ρ_{*s} is the normalized gyroradius. Experimental data for the barrier width from DIII-D and C-Mod, however, did

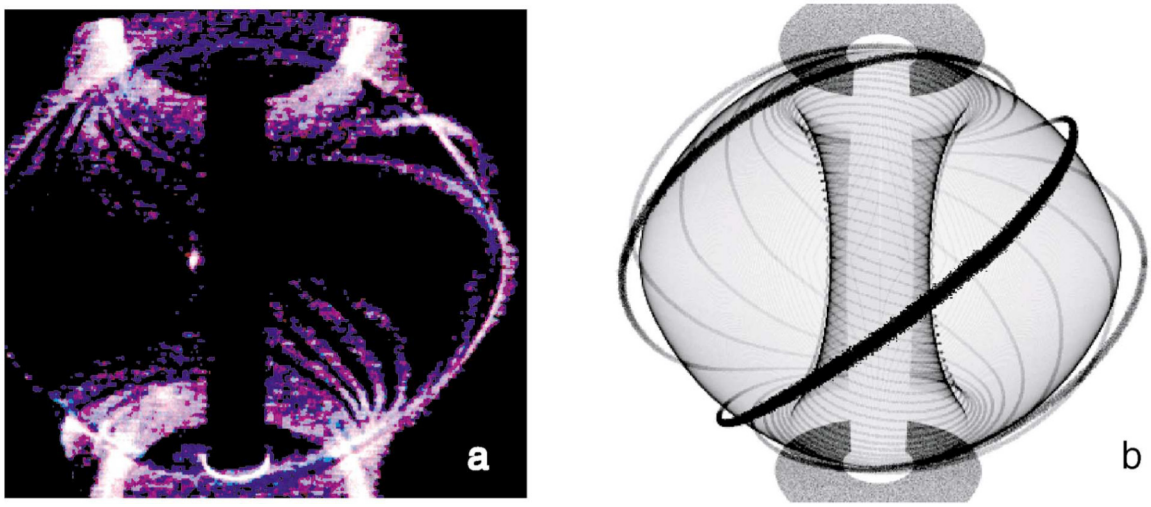

Fig. 7. (a) High-speed video image of the MAST plasma obtained at the start of an ELM. (b) The predicted structure of an ELM in the MAST tokamak plasma geometry, based on the nonlinear ballooning mode history [116]. *[Reprinted courtesy of A. Kirk, et al., Phys. Rev. Lett.* ***92****, 245002 (2000), American Institute of Physics.]*

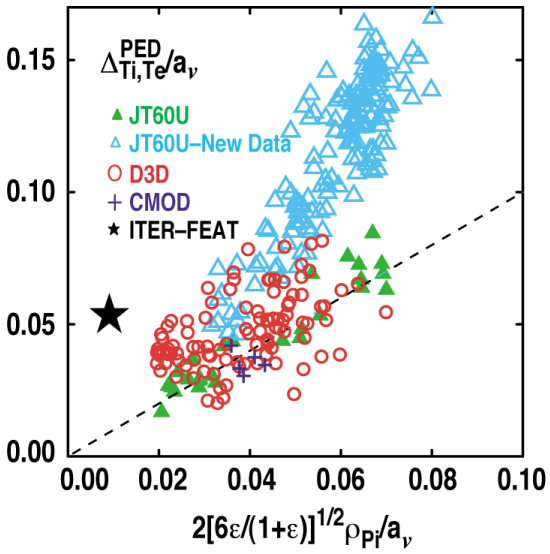

Fig. 8. Normalized temperature widths and normalized banana widths for several machines [130]. *[Reprinted courtesy of T.H. Osborne, et al., Proc. 19th IAEA Fusion Energy Conf., Lyon, France (Vienna: IAEA, 2002) Paper CT-3, International Atomic Energy Agency.]*

not correlate well with the normalized gyroradius [130]. Furthermore, the dependence of the barrier width on ρ_{*s} is also inconsistent with more recent results from DIII-D in which the barrier width was invariant to a significant change (by a factor of 2) in ρ_{*s} [124]. Therefore, this approach for predicting the spatial structure of the ETB needs further improvement before it can be applied to future devices. Furthermore, data for Type I ELMy H-mode plasmas in ASDEX Upgrade shows a correlation between the decay lengths for the edge electron density and temperature [i.e. $\eta_e = d(\ell n T_e))/d(\ell n n_e) \sim 2$] which could be consistent with critical η_e behavior for ETG and drift mode turbulence [138].

There still exist large uncertainties in predicting the spatial structure of the ETB using mechanisms for suppressing turbulent transport at the plasma edge. This is partly due to an incomplete understanding of the processes that generate the radial electric field and the flow shear at the plasma edge. Coupled with this are the influences of MHD instabilities and atomic processes, such as the neutral penetration, that further complicate the evaluation of the spatial structure. Therefore, a model for the ETB structure would need to take account of all these effects to be truly predictive. This is an important challenge for the edge theory and modeling community and one that needs to be addressed.

Future fusion devices would benefit from having plasmas with ETBs (and their inherent high energy confinement), but which do not contain large ELMs which can erode the divertor surfaces due to their high peaked heat loads. ETBs can now be formed that provide good particle control, but which do not exhibit ELM activity. Examples of these ELM-free H-mode ETBs are the enhanced D_α (EDA) mode in C-Mod [139, 140], the quiescent H-mode (QH-mode) in DIII-D [141], ASDEX Upgrade [142], JET [143] and JT-60U [144] and the high recycling steady (HRS) H-mode in JFT-2M [145].

All these ELM-free ETBs contain continuous, localized MHD fluctuations which provide the increased particle transport through the barrier, which is required for density control. In C-Mod, these fluctuations [referred to as quasi-coherent (QC)-modes] have been observed on density, magnetics and electrostatic potential diagnostics and have been localized to a region of a few millimeters near the bottom of the density gradient in the ETB [146, 147].

The QC-mode drives substantial particle flux in the edge and appears to be the cause of the increased edge particle transport in the EDA H-mode. The mode has a peak frequency that lies in the range $50 - 120\,\mathrm{kHz}$ and a fairly short poloidal wavelength with wave number $k_\theta \sim 1.2 - 4.0\,\mathrm{cm}^{-1}$. The edge particle transport correlates well with the mode amplitude. Measurements of the fluctuation characteristics suggest that the mode may be some type of resistive drift ballooning mode. The HRS H-mode in JFT-2M is very similar to the EDA H-mode in C-Mod. Both regimes are prevalent at higher q_{95} and high collisionality. The HRS H-mode is characterized by the presence of coherent magnetic fluctuations between $10 - 100\,\mathrm{kHz}$ located in the high gradient region of the ETB [148, 149].

The QH-mode ETB in DIII-D, which requires neutral beam injection counter to the plasma current direction, is typically marked by the presence of coherent electromagnetic fluctuations called edge harmonic oscillations (EHOs) with multiple harmonics (with a base frequency of $\sim 6 - 10\,\mathrm{kHz}$) with a variable mix of toroidal mode numbers from typically 1 to 10 and a poloidal wavelength of $\sim$1 m [141]. Edge harmonic oscillations have also been observed in the QH-mode of ASDEX Upgrade [142], JET [143], and JT-60U [144]. Density control is achieved through increased edge particle transport caused by the EHOs (although energy transport is not significantly increased). The mechanism that causes the EHO is, as yet, unknown. It should be noted that measurements of the edge radial field, E_r, profiles indicate that QH-mode plasmas have 2-3 times deeper E_r wells inside the last closed flux surface compared to standard ELM-free H-modes with co-NBI or to ELMing H-mode with counter-NBI [150], which may have a bearing on the formation of the EHO. Stability analysis indicates that the QH-mode edge barrier is marginally stable to current driven modes [151].

It is important to note that all these quiescent ELM-free H-mode regimes have edge pedestal structures similar to those of the ELMing plasmas, so energy confinement and plasma performance are not diminished compared to an ELMing ETB.

IV. Conclusions

The edge transport barrier in magnetic fusion plasmas plays an extremely important role in the overall performance of the whole plasma. The dynamics and structure of the ETB, controlled by the transport and stability processes at the plasma edge, affect not only the plasma core behavior, but also the characteristics of the scrape-off layer and the divertor conditiions. A key aspect in the formation of ETBs is determining and understanding the mechanisms that can stabilize plasma turbulence and, thereby, reduce turbulence-driven transport at the plasma edge. Substantial progress has been made on determining the stabilization mechanism through concerted efforts based on theoretical and numerical modeling studies with detailed experimental measurements of the plasma edge. An important outcome of these coordinated investigations is that it is now widely accepted that $E \times B$ flow shear stabilization of turbulence (with the subsequent reduction in transport) plays a critical role in the formation of ETBs. Consequently, turbulent transport at the edge can be directly affected by changing the $E \times B$ flow shear, as has been demonstrated, for example, in biased electrode experiments. However, the processes for the initial creation of the $E \times B$ flow shear in spontaneously produced ETBs are, as yet, not fully resolved. Various processes (e.g., ion-orbit loss, Stringer spin-up, Reynolds stress, neutral particle effects, etc.) have been suggested.

Both theoretical and experimental work has brought drift wave zonal flows to the forefront as a viable mechanism by which zonal $E \times B$ flow and drift wave turbulence can self-regulate each other in a spontaneous manner and may trigger the large bifurcation in the mean $E \times B$ flow shear needed to stabilize edge turbulence. Measurements of Reynolds stress, which drives zonal flows, have been made in several devices. Bicoherence measurements at the plasma edge have indicated rapid changes prior to the ETB formation consistent with a transient Reynolds stress driven zonal flow shear. Measurements of the higher frequency zonal flows called GAMs have also been made whereby their spatial structure has been determined at the plasma edge. These experimental studies, coupled with the theoretical basis for zonal flows, are examples of progress towards understanding turbulent trans-

port at the plasma edge. However, further progress will require significant improvements in the temporal and spatial resolution of edge diagnostics and satisfying these requirements needs to be a critical element of future work in this area.

There still exist large uncertainties in predicting the spatial structure of the ETB, especially the barrier width, using mechanisms for reducing turbulent transport at the plasma edge. This is primarily the result of an incomplete understanding of the processes that generate the flow shear at the plasma edge. Furthermore, the evaluation of the width scaling, for example, are complicated by the influences of atomic processes and MHD instabilities once the barrier is formed. Ultimately, a predictive model of the ETB has to take into account and incorporate the physics of all of the above processes to be truly effective. This is an important challenge that needs coordinated efforts in all disciplines of plasma physics (theoretical, modeling, and experimental) to be successfully met.

References

[1] Wagner F., *et al.*, Phys. Rev. Lett. **49** (1982) 1408.

[2] ITER Physics Basis Document, Nucl. Fusion **39** (1999) 2136.

[3] Lehnert B., Phys. Fluids **9** (1996) 1367.

[4] Shaing K.C., Crume E.C., Phys. Rev. Lett. **63** (1989) 2369.

[5] Itoh S.-I., *et al.*, Plasma Phys. and Control. Nuclear Fusion Research, Vol. 12 (Proc. 12th Int. Conf., IAEA, Nice, 1989) p. 23.

[6] Biglari H., Diamond P.H., Terry P.W., Phys. Fluids B **2** (1990) 1.

[7] Hassam A., Comments Plasma Phys. and Control. Fusion **14** (1991) 275.

[8] Shaing K.C., Crume, Jr. E.C., Houlberg W.A., Phys. Fluids **2** (1990) 1492,

[9] Bishop C.M., Nucl. Fusion **26** (1986) 1063.

[10] Bishop C.M., Nucl. Fusion **27** (1987) 1765.

[11] Connor J.W., Hastie R.J., Wilson H.R., Miller R.L., Phys. Plasmas **5** (1998) 2687.

[12] Wilson H.R., Connor J.W., Field A., Fielding S.J., Miller R.L., Lao L.L., Ferron J.R., Turnbull A.D., Phys. Plasmas **6** (1999) 1925.

[13] Drake J.F., Lau Y.T., Guzdar P.N., Hassam A.B., Novakovski S.V., Rogers B., Zeiler A., Phys. Rev. Lett. **77** (1996) 494.

[14] Rogers B.N., Drake J.F., Phys. Rev. Lett. **79** (1997) 229.

[15] Rogers B.N., Drake J.F., Zeiler A., Phys. Rev. Lett. **81** (1998) 4396.

[16] Zeiler A., Biskamp D., Drake J.F., Guzdar P.N., Phys. Plasmas **3** (1996) 2951.

[17] Zeiler A., Drake J.F., Biskamp D., Phys. Plasmas **4** (1997) 991.

[18] Scott B., *et al.*, Fusion Energy (Proc. 16th Int. Conf., Montreal, 1996) Vol. 2 (Vienna IAEA) p. 649.

[19] Scott B., Plasma Phys. and Control. Fusion **40** (1998) 823.

[20] Pogutse O., *et al.*, Proc. 24th EPS Conf. on Controlled Fusion and Plasma Physics, Berchtesgaden, Germany, Vol. 21A, Part III (Euro. Physical Society, 1997) p. 1041.

[21] Pogutse O., Igitkhanov Yu., Czech. J. Plasma Physics **48** (supp. S2) (1998) 39.

[22] Kerner W., Igitkhanov Yu., Janeschitz G., Pogutse O., Contrib. Plasma Physics **38** (1998) 118.

[23] Zohm H., *et al.*, Fusion Energy (Proc. 16th Int. Conf., Montreal, 1996) Vol. 1 (Vienna: IAEA) p. 439.

[24] Igitkhanov Yu., Janeschitz, G., Pacher G.W., Sugihara M., Pacher H.D., Post D.E., Solano E., Lingertat J., Loarte A., Osborne T., Pogutse O.P., Shimada M., Suttrop W., Plasma Phys. Control. Fusion **40** (1998) 837.

[25] Fielding S.J., *et al.*, Control. Fusion and Plasma Phys., Vol. 22C (Proc. 25th EPS Conf., Prague, Czech Republic, 1998) p. 838.

[26] Gohil P., Baylor L.R., Jernigan T.C., Burrell K.H., Carlstrom T.N., Phys. Rev. Lett. **86** (2001) 644.

[27] Hubbard A.E., Boivin R.L., Drake J.F., Greenwald M., In Y., Irby J.H., Rogers B.N., Snipes J.A., Plasma Phys. and Control. Fusion **40** (1998) 689.

[28] Carlstrom T.N., Burrell K.H., Groebner R.J., Leonard A.W., Osborne T.H., Thomas D.M., Nucl. Fusion **39** (1999) 1941.

[29] Field A., *et al.*, Proc. 26th EPS Conf. on Controlled Fusion and Plasma Physics, Maastricht, Netherlands, Vol. 23J (Euro. Physical Society, 1999) p. 273.

[30] Janeschitz G., *et al.*, Proc. 24th EPS Conf. on Controlled Fusion and Plasma Physics, Berchtesgaden, Germany, Vol. 21A, Part III (Euro. Physical Society, 1997) p. 993.

[31] Igitkhanov Yu., et al., Plasma Phys. Control. Fusion **40** (1998) 837.

[32] Itoh S.-I., Itoh K., Phys. Rev. Lett. **60** (1988) 2276.

[33] Waltz R.E., Kerbel G.D., Milovich J., Phys. Plasmas **1** (1994) 2229.

[34] Waltz R.E., Kerbel G.D., Milovich J.,, Hammett G.W., Phys. Plasmas **2** (1995) 2408.

[35] Carreras B.A., Sidikman K., Diamond P.H., Terry P.W., Garcia L., Phys. Fluids **B4** (1992) 3115.

[36] Rettig C.L., et al., Phys. Plasmas **5** (1998) 1727.

[37] Burrell K.H., Austin M.E., Greenfield C.M., Lao L.L., Rice B.W., Staebler G.M., Stallard B.W., Plasma Phys. and Control. Fusion **40** (1998) 1589.

[38] Schissel D.P., Greenfield C.M., DeBoo J.C., Lao L.L., Lazarus E.A., Navratil G.A., Rice B.W., Staebler G.M., Stallard B.W., Strait E.J., St. John H.E., Austin M.E., Burrell K.H., Casper T.A., Baker D.R., Chan V.S., Doyle E.J., Ferron J.R., Forest C.B., Gohil P., Groebner R.J., Heidbrink W.W., Hong R.-M., Howald A.W., Hsieh C.-L., Hyatt A.W., Jackson G.L., Kim J., Lasnier C.J., Leonard A.W., Lohr J., La Haye R.J., Maingi R., Miller R.L., Murakami M., Osborne T.H., Petty C.C., Rettig C.L., Rhodes T.L., Sabbagh S., Scoville J.T., Snider R.T., Stambaugh R.D., Stockdale R.E., Taylor P.L., Taylor T.S., Thomas D.M., Wade M.R., Waltz R.E., Wood R.D., Whyte D.G., Proc. 16th Fusion Energy Conf., Montreal, Canada, Vol. 1 (Vienna: IAEA, 1997) p. 463.

[39] Esposito B., et al., Proc. 28th EPS Conf. on Controlled Fusion and Plasma Physics, Madeira, Portugal, Vol. 25A (Euro. Physical Society, Lisboa, 2001) p. 553.

[40] Crisanti F., Esposito B., Gormezano C., Tuccillo A., Bertalot L., Giroud C., Gowers C.W., Prentice R., Zastrow K.-D., Zerbini M., Nucl. Fusion **41** (2001) 883.

[41] Mazzucato E., Batha S.H., Beer M., Bell M., Bell R.E., Budny R.V., Bush C., Hahm T.S., Hammet G.W., Levinton F.M., Nazikian R., Park H., Rewoldt G., Schmidt G.I., Synakowski E.J., Tang W.M., Taylor G., Zarnstorff M.C., Phys. Rev. Lett. **77** (1996) 3145.

[42] Synakowski E.J., et al., Phys. Plasmas **4** (1997) 1736.

[43] Hahm T.S., Burrell K.H., Phys. Plasmas **2** (1995) 1648.

[44] Gohil P., Burrell K.H., Carlstrom T.N., Nucl. Fusion **38** (1998) 93.

[45] Burrell K.H., Proc. 15th Int. Conf. on Plasma Physics and Controlled Fusion, Vol. 1 (Vienna: IAEA, 1995) p. 221.

[46] Moyer R.A., Burrell K.H., Carlstrom T.N., Coda S., Conn R.W., Doyle E.J., Gohil P., Groebner R.J., Kim J., Lehmer R., Peebles W.A., Porkolab M., Rettig C.L., Rhodes T.L., Seraydarian R.P., Stockdale R., Thomas D.M., Tynan G.R., Watkins J.G., Phys. Plasmas **2** (1995) 2397.

[47] Burrell K.H., et al., Rev. Sci. Instrum. **72** (2001) 906.

[48] Moyer R.A., Rhodes T.L., Rettig C.L., Doyle E.J., Burrell K.H., Cuthbertson J., Groebner R.J., Kim K.W., Leonard A.W., Maingi R., Porter G.D., Watkins J.G., Plasma Phys. Control. Fusion **41** (1999) 243.

[49] Gohil P., Burrell K.H., Doyle E.J., Groebner R.J., Kim J., Seraydarian R.P., Nucl. Fusion **34** (1994) 1057.

[50] Coda S., et al., Phys. Lett. A **273** (2000) 125.

[51] Coda S., *et al.*, Proc. 24th EPS Conf. on Controlled Fusion and Plasma Physics, Berchtesgaden, Germany, Vol. 21A, Part III (Euro. Physical Society, 1997) p. 1141.

[52] Ida K., Hidekuma S., Miura Y., Fujita T., Mori M., Zuzuki N., Yamauchi T., and the JFT-2M Group, Phys. Rev. Lett. **65** (1990) 1364.

[53] Ido T., Kamiya K., Miura Y., Hamada Y., Nishizawa A., Kawasumi Y., Plasma Phys. and Control. Fusion **42** (2000) A309.

[54] Miura Y., Ido T., Kamiya K., Hamada Y., JFT-2M Group, Nucl. Fusion **41** (2001) 973.

[55] Carolan P., *et al.*, Proc. 28th EPS Conf. on Controlled Fusion and Plasma Physics, Madeira, Portugal, Vol. 25A (Euro. Physical Society, Lisboa, 2001) p. 1821.

[56] Field A.R., Fussmann G., Hofmann J.V., Nucl. Fusion **32** (1992) 1191.

[57] Wagner F., Baldzuhn J., Brakel R., Burhenn R., Erckmann V., Estrata T., Grigull P., Hartfuss H.J., Herre G., Hirsch M., Hofmann J.V., Jaenicke R., Rudyj A., Stroth U., Weller A., the W7-AS Teams, Plasma Phys. and Control. Fusion **36** (1994) A61.

[58] Rudakov D.L., Shats M.G., Harris J.H., Blackwell B.D., Plasma Phys, and Control. Fusion **43** (2001) 559.

[59] Taylor R.J., Brown M.L., Fried B.D., Grote H., Liberati, J.R., Morales G.J., Pribyl P., Darrow D., Ono M., Phys. Rev. Lett. **63** (1989) 2365.

[60] Askinazi L.G., Golant V.E., Lebedev S.V., Rozhanskij V.A., Tendler M., Nucl. Fusion **32** (1992) 271.

[61] Weynants R.R., Jachmich S., Van Oost G., Plasma Phys. and Control. Fusion **40** (1998) 635.

[62] Boedo J.A., et al., Phys. Rev. Lett. **84** (2000) 2630.

[63] Jachmich S., Van Oost G., Weynants R.R., Boedo J.A., Plasma Phys. and Control. Fusion **40** (1998) 1105.

[64] Burrell K.H., et al., Phys. Plasmas **6** (1999) 441.

[65] Jackson G.L., Winter J., Taylor T.S., Burrell K.H., DeBoo J.C., Greenfield C.M., Groebner R.J., Hodapp H., Holtrop K., Lazarus E.A., Lao L.L., Lippman S.I., Osborne T.H., Petrie T.W., Phillips J., James R., Schissel D.P., Strait E.J., Turnbull A.D., West W.P., and DIII-D Team, Phys. Rev. Lett. **67** (1991) 3098.

[66] Jackson G.L., Winter J., Taylor T.S., Greenfield C.M., Burrell K.H., Carlstrom T.N., DeBoo J.C., Doyle E.J., Groebner R.J., Lao L.L., Rettig C., Schissel D.P., Strait E.J., DIII-D Research Team, Phys. Fluids **B4** (1992) 2181.

[67] La Haye R.J., Groebner R.J., Hyatt A.W., Scoville J.T., Nucl. Fusion **33** (1993) 349.

[68] La Haye R.J., Osborne T.H., Rettig C.L., Greenfield C.M., Hyatt A.W., Scoville J.T., Nucl. Fusion **35** (1995) 988.

[69] Hassam A.B., Antonsen T.M., Drake J.F., Liu S.C., Phys. Rev. Lett. **66** (1991) 309.

[70] Diamond P.H., Kim Y.B., Phys. Fluids **3** (1991) 1626.

[71] Lin Z., Hahm T.S., Lee W.W., Tang W.M., White R.B., Science **281** (1998) 1835.

[72] Kim J., Burrell K.H., Gohil P., Groebner R.J., Kim Y.-B., St. John H.E., Seraydarian R.P., Wade M.R., Phys. Rev. Lett. **72** (1994) 2199.

[73] Diamond P.H., Itoh S.-I., Itoh K., Hahm T.S., Plasma Phys. and Control. Fusion **47** (2005) R35.

[74] Hinton F.L., Rosenbluth M.N., Plasma Phys. and Control. Fusion **41** (1999) A653.

[75] Itoh K., Plasma Phys. and Control. Fusion **47** (2005) 451.

[76] Fujisawa A., *et al.,* Proc. 31st EPS Conf. on Controlled Fusion and Plasma Physics, London, United Kingdom (Euro. Physical Society, 2004) paper O2-04.

[77] Fujisawa A., Itoh K., Iquchi H., Matsuoka K., Okamura S., Shimizu A., Minami, T., Yoshimura Y., Nagaoka K., Takahashi C., Kojima M., Nakano H.., Ohasima S., Nishimura S., Isobe M., Suzuki C., Akiyama T., Ida K., Toi K., Itho S.-I., Diamond P.H., Phys. Rev. Lett. **93** (2004) 165002.

[78] Tynan G.R., Moyer R.A., Burin M.J., Holland C., Phys. Plasmas **8** (2001) 2691.

[79] Moyer R.A., Tynan G.R., Holland C., Burin M.J., Phys. RB., Hirsch M., Hartfuss H.J., Carreras B.A., Phys. Rev. Lett. **87** (2001) 135001.

[80] Diamond P.H., Rosenbluth M.N., Sanchez E., Hidalgo C., Van Milligen B., Estrata T., Branas Phys. Rev. Lett. **84** (2000) 4842.

[81] Xu Y., et al., Phys. Rev. Lett. **84** (2000) 3867.

[82] Hildago C., et al., Phys. Rev. Lett. **83** (1999) 2203.

[83] Tynan G.R., et al., Plasma Phys. and Control. Fusion **48** (2006) S51.

[84] Xu G.S., Wan B.N., Li J., Proc. 20th IAEA Fusion Energy Conf. (Vilamoura, Portugal, 2004) EX/8-4Rb, IAEA-CSP-5/CD Vienna.

[85] Vianello N., Spada E., Antoni V., Spolaore M., Serianni G., Regnoli G., Cavazzana R., Bergsaker H., Drake J.R., Phys. Rev. Lett. **94** (2005) 135001.

[86] Guzdar P.N., Kleva R.G., Groebner R.J., Gohil P., Phys. Rev. Lett. **89** (2002) 265004.

[87] Nagashima Y., et al., Phys. Rev. Lett. **95** (2005) 095002.

[88] Ido T., *et al.*, Proc. of 20th IAEA Conf. on Fusion Energy (Portugal: IAEA, 2004) Paper EX4-6Rb.

[89] Jakubowski M., et al., Phys. Rev. Lett. **89** (2000) 265003.

[90] Conway G., *et al.,* Plasma Phys. and Control. Fusion **47** (2005) 1165.

[91] McKee G.R., Fonck R.J., Jakubowski M., Burrell K.H., Hallatschek K., Moyer R.A., Rudakov D.L., Nevins W., Porter G.D., Schoch P., Xu X., Phys. Plasmas **10** (2003) 1712.

[92] McKee G.R., Fonck R.J., Jakubowski M., Burrell K.H., Hallatschek K., Moyer R.A., Nevins W., Rudakov D.L., Xu X., Plasma Phys. and Control. Fusion **45** (2003) A477.

[93] McKee G.R., et al., Plasma Phys. and Control. Fusion **48** (2006) S123.

[94] Ido T., et al., Plasma Phys. and Control. Fusion **48** (2006) S41.

[95] Hubbard A.E., Carreras B.A., Boivin R.L., Hughes J.W., Marmar E.S., Mossessian D., Wukitch S.J., Plasma Phys. and Control. Fusion **44** (2002) A359.

[96] Righi E., Campbell D.J., Conway G.D., Hawkes N.C., Horton L.D., Maggi C.F., Saiben G., Sartori R., Zastrow K.-D., Plasma Phys. and Control. Fusion **42** (2000) A199.

[97] Andrew Y., Hawkes N.C., O'Mullane M.G., Sartori R., Beurskens M.N.A., Coffey I., Joffrin E., Loarte A., McDonald D.C., Prentice R., Saibene G., Suttrop W., Zastrow K.-D., JET EFDA Contributors, Plasma Phys. and Control. Fusion **46** (2004) 337.

[98] Ryter F., H-mode Threshold Database Group, Plasma Phys. and Control. Fusion **44** (2002) A415.

[99] Carlstrom T.N., Groebner R.J., Fenzi C., McKee G.R., Moyer R.A., Rhodes T.l., Plasma Phys. and Control. Fusion **44** (2002) A333.

[100] Akers R.J., Ahn J.W., Antar G.Y., Appel L.C., Applegate D., Brickley C., Bunting C., Carolan P.G., Challis C.D., Conway N.J., Counsell G.F., Dendy R.O., Dudson B., Field A.R., Kirk A., Lloyd B., Meyer H.F., Morris A.W., Patel A., Roach C.M., Rohzansky V., Sykes A., Taylor D., Tournianski M.R., Valovic&breve M., Wilson H.R., Axon K.B., Buttery R.J., Ciric D., Cunningham G., Dowling J., Dunstan M.R., Gee S.J., Gryaznevich M.P., Helander P., Keeling D.L., Knight P.J., Lott F.,

Loughlin M.J., Manhood S.J., Martin R., McArdle G.J., Price M.N., Stammers K., Storrs J., Walsh M.J., the MAST and NBI Team, Plasma Phys. and Control. Fusion **45** (2003) A175.

[101] Bush E.C., Bell M.G., Bell R.E., Boedo J., Fredrickson E.D., Kaye S.M., Kubota S., LeBlanc B.P., Maingi R., Maqueda R.J., Sabagh S.A., Soukhanovskii V.A., Stutman D., swain D.W., Wilgen J.B., Zweben S.J., Davis W.M., Gates D.A., Johnson D.W., Kaita R., Kugel H.W., Lee K.C., Mastrovito D., Medley S., Menard J.E., Mueller D., Ono M., Paoletti F., Park H., Paul S.J., Peng Y.-K.M. Raman R., Roney P.G., Roquemore A.L., Skinner C.H., Synakowski E.J., Taylor G., Phys. Plasmas **10** (2003) 1755.

[102] Owen L.W., Carreras B.A., Maingi R., Mioduszewski P.K., Carlstrom T.N., Groebner R.J., Plasma Phys. and Control. Fusion **40** (1998) 717.

[103] Fukuda T., Takizuka T., Tsuchiya K., Kamada Y., Nagashima K., sato M., Takenaga H., Ishida S., Konoshima S., Higashijima S., Tobita K., Kikuchi M., Mori M., Nucl. Fusion **37** (1997) 1199.

[104] Takizuka T., ITPA H-mode Power Threshold Database Working Group, Plasma Phys. and Control. Fusion **46** (2004) A227.

[105] Coppi B., Shanky N., Nucl. Fusion **21** (1981) 1363.

[106] Janeschitz G., *et al.*, in Controlled Fusion and Plasma Physics (Proc. 26th EPS Conf., Maastricht, The Netherlands, Vol. 23J (Geneva: EPS, 1999) p. 1445.

[107] Hatae T., Sugihara M., Hubbard A.E., Igitkhanov Yu., Kamada Y., Janeschitz G., Horton L.D., Ohyabu N., Osborne T.H., Osipenko M., Suttrop W., Urano H., Weisen H., Nucl. Fusion **41** (2001) 285.

[108] Kotschenreuther M., *et al.*, Proc. 16th IAEA Fusion Energy Conf., Montreal, Canada, Vol. 2 (Vienna: IAEA, 1997) p. 371.

[109] Waltz R.E., *et al.*, Proc. 16th IAEA Fusion Energy Conf., Montreal, Canada, Vol. 2 (Vienna: IAEA, 1997) p. ???.

[110] Suttrop W., Plasma Phys. and Control. Fusion **42** (2000) A1.

[111] Lao L.L., Plasma Phys. and Control. Fusion **42** (2000) A51.

[112] Wilson H.R., Connor J.W., Field A.R., Fielding S.J., Hastie R.J., Miller R.L., Taylor J.B., Nucl. Fusion **40** (2000) 713.

[113] Snyder P.B., Wilson H.R., Ferron J.R., Lao L.L., Leonard A.W., Osborne T.H., Turnbull A.D., Mossessian D., Murakami M., Xu X.Q., Phys. Plasmas **9** (2002) 2037.

[114] Cowley S.C., Wilson H., Hurricane O., Fong B., Plasma Phys. and Control. Fusion **45** (2003) A31.

[115] Wilson H.R., Cowley S.C., Phys. Rev. Lett. **92** (2004) 175006.

[116] Kirk A., Wilson H.R., Counsell G.F., Akers R., Arends E., Cowley S.C., Dowling J., Lloyd B., Price M., Walsh M., Phys. Rev. Lett. **92** (2004) 245002. Vol. 2 (Vienna: IAEA, 1997) p. 385.

[117] Lang P.J., *et al.*, Proc. 30th EPS Conf. on Controlled Fusion and Plasma Physics, Vol. 27A (St Petersburg, EPS, 2003) Paper 1.129.

[118] Urano H., et al., Plasma Phys. and Control. Fusion **46** (2004) A315.

[119] Evans T.E., et al., Phys. Rev. Lett. **92** (2004) 235003.

[120] Burrell K.H., et al., Plasma Phys. and Control. Fusion **47** (2005) B37.

[121] Sakamoto Y., and the JT-60 Team, Plasma Phys. and Control. Fusion **47** (2005) B337.

[122] Fielding S.J., *et al.*, Proc. 28th EPS Conf. on Controlled Fusion and Plasma Physics, Vol. 25A (Madeira, EPS, 2001) p. 1825.

[123] Degeling A.W., et al., Plasma Phys. and Control. Fusion **45** (2003) 1637.

[124] Fenstermacher M.E., Osborne T.H., Leonard A.W., Snyder P.B., Thomas D.M., Boedo J.A., Casper T.A., Groebner R.J., Groth M., Kempenaars M.A.H., Loarte A., McKee G.R., Meyer W.M., Saibene G., VanZeeland M.A., Xu X.Q., Zeng L., the DIII-D Team, Nucl. Fusion **45** (2005) 1493.

[125] Kinsey J.E., Staebler G.M., Waltz R.E., Phys. Plasmas **12** (2005) 052503.

[126] Itoh S.-I., Itoh K., Nucl. Fusion **29** (1989) 1031.

[127] Shaing K.C., Hsu C.T., Phys. Plasmas **2** (1995) 1801.

[128] Itoh K., Plasma Phys. and Control. Fusion **36** (1994) A307.

[129] Hatae T., Kamada Y., Ishida S., Fukuda T., Takizuka T., Shirai H., Koide Y., Kikuchi M., Yoshida H., Naito O., Plasma Phys. and Control. Fusion **40** (1998) 1073.

[130] Osborne T.H., *et al.*, Proc. 19th IAEA Fusion Energy Conf., Lyon, France (Vienna: IAEA, 2002) Paper CT-3.

[131] Hinton F.L., Kim J., Kim Y.-B., Brizard A., Burrell K.H., Phys. Rev. Lett. **72** (1994) 1216.

[132] Shiang K.C., Phys. Fluids **B4** (1992) 290.

[133] Breger P., Flewin C., Zastrow K.-D., Davies S.J., Hawkes N.C., Konig R.W.T., Pietrzyk Z.A., Porte L., Summers D.D.R., von Hellermann M.G., Plasma Phys. and Control. Fusion **40** (1998) 347.

[134] Ida K., Miura Y., Itoh K., Itoh S.-I., Fukuyama A., Plasma Phys. and Control. Fusion **36** (1994) A279.

[135] Groebner R.J., Mahdavi M.A., Osborne T.H., Porter G.D., Plasma Phys. and Control. Fusion **44** (2002) A265.

[136] Waltz R.E., Staebler G.M., Dorland W., Hammet G.W., Kotschenreuther M., Konings J.A., Phys. Plasmas **4** (1997) 2482.

[137] Kinsey J.E., Staebler G.M., Waltz R.E., Phys. Plasmas **9** (2002) 1676.

[138] Neuhauser J., Coster D., Fahrbach H.U., Fuchs J.C., Haas G., Herrman A., Horton L., Jakobi M., Kallenbach A., Laux M., Kim J.W., Kurzan B., Müller H.W., Murmann H., Neu R., Rohde V., Sandmann W., Suttrop W., Wolfrum E., and the ASDEX Upgrade Team, Plasma Phys. and Control. Fusion **44** (2002) 855.

[139] Greenwald M., et al., Nucl. Fusion **37** (1997) 793.

[140] Takase Y., et al., Phys. Plasmas **4** (1997) 1647.

[141] Burrell K.H., et al., Phys. Plasmas **8** (2001) 2153.

[142] Suttrop W., et al., Plasma Phys. and Control. Fusion **46** (2004) A151.

[143] Suttrop W., et al., Nucl. Fusion **45** (2005) 721.

[144] Oyama N., *et al.*, Proc. 20th Int. Fusion Energy Conf., Vilamoura, Portugal (Vienna: IAEA, 2004) Paper EX/2-1.

[145] Kamiya K., et al., Nucl. Fusion **43** (2003) 1214.

[146] Snipes J.A., et al., Plasma Phys. and Control. Fusion **43** (2001) L23.

[147] Mazurenko A., et al., Phys. Rev. Lett. **89** (2002) 225004.

[148] Kamiya K., et al., Plasma Phys. and Control. Fusion **46** (2004) A157.

[149] Nagashima N., et al., Plasma Phys. and Control. Fusion **46** (2004) A381.

[150] Gohil P., et al., Plasma Phys. and Control. Fusion **45** (2003) 601.

[151] Burrell K.H., et al., Phys. Plasmas **12** (2005) 056121,

Acknowledgment

This work was supported in part by the U.S. Department of Energy under DE-FC02-04ER54698.